

## Room-temperature ferromagnetism in undoped GaN and CdS semiconductor nanoparticles

C. Madhu, A. Sundaresan,\* and C. N. R. Rao†

*Chemistry and Physics of Materials Unit and Department of Science and Technology Unit on Nanoscience, Jawaharlal Nehru Centre for Advanced Scientific Research, Jakkur P.O., Bangalore 560 064, India*

(Received 11 February 2008; revised manuscript received 11 April 2008; published 29 May 2008)

Room-temperature ferromagnetism has been observed in undoped GaN and CdS semiconductor nanoparticles of different sizes with the average diameter in the range 10–25 nm. These nanoparticles were synthesized by simple routes and thoroughly characterized by various techniques. Magnetization measurements at room temperature show that these nanoparticles are ferromagnetic with a saturation magnetization of  $\sim 10^{-3}$  emu/gm, which is comparable to that observed in nanoparticles of nonmagnetic oxides. On the other hand, agglomerated particles of GaN and CdS exhibit diamagnetism or ferromagnetism with small saturation moments. Furthermore, the saturation magnetic moment decreases with the increase in particles size, suggesting that ferromagnetism is due to the defects confined to the surface of the nanoparticles, while the core of the particles remains diamagnetic. The observation of ferromagnetism is consistent with the prediction that Ga vacancies in GaN give rise to a ferromagnetic ground state.

DOI: [10.1103/PhysRevB.77.201306](https://doi.org/10.1103/PhysRevB.77.201306)

PACS number(s): 75.70.Rf, 75.60.Ej, 78.67.Bf

Since the prediction of ferromagnetism in Mn-doped GaN by Dietl *et al.*,<sup>1</sup> there have been several reports of observation of room-temperature ferromagnetism in various forms of the GaN semiconductor doped with Mn and other magnetic elements.<sup>2–5</sup> Among the various forms, thin films of Mn-doped GaN have been investigated because of its potential application in spintronics.<sup>1,6,7</sup> However, there has been a controversy over the existence of ferromagnetism in this material. While thin films of Mn-doped GaN prepared by some groups have been reported to be ferromagnetic, there are reports of paramagnetic behavior in this material.<sup>8–10</sup> There are also suggestions that the observed ferromagnetism may arise from possible impurity phases such as Ga-Mn or Mn-N alloys.<sup>11,12</sup> Meanwhile, other forms such as nanowires and nanocrystals of Mn-doped GaN have also been reported to exhibit ferromagnetism.<sup>13,14</sup>

It is interesting to note that thin films of several nonmagnetic oxides such as HfO<sub>2</sub>, TiO<sub>2</sub>, In<sub>2</sub>O<sub>3</sub>, ZnO, and SnO<sub>2</sub> have been reported to show room temperature ferromagnetism.<sup>15,16,18–20</sup> While oxygen vacancies have been suggested to be the origin of ferromagnetism in these oxides, theoretical calculations on HfO<sub>2</sub> have shown that ferromagnetism arises because of Hf vacancies.<sup>21</sup> Recently, we have reported room-temperature ferromagnetism in the nanoparticles of nonmagnetic oxides such as CeO<sub>2</sub>, Al<sub>2</sub>O<sub>3</sub>, ZnO, In<sub>2</sub>O<sub>3</sub>, and SnO<sub>2</sub>.<sup>22</sup> The origin of magnetism in these materials has been suggested to be due to oxygen vacancies at the surface of the nanoparticles. It was also pointed out that the ferromagnetism may be a universal characteristic of nanoparticles of metal oxides. Subsequently, we have demonstrated that the surface ferromagnetism can exist even in the well-known YBa<sub>2</sub>Cu<sub>3</sub>O<sub>y</sub> superconductor nanoparticles at least down to the superconducting transition temperature.<sup>23</sup> Some of the nitride superconductors such as NbN and  $\delta$ -MoN were also shown to exhibit ferromagnetism above the superconducting transition temperature.<sup>23</sup> Similarly, the surface ferromagnetism could be combined with the ferroelectricity in the nanoparticles of well-known ferroelectric material BaTiO<sub>3</sub>, where the ferroelectricity comes from the core and the ferromagnetism is confined to the surface.<sup>24</sup> Considering the im-

portance of magnetic semiconductor in the spintronics, we have investigated the magnetic properties of nanoparticles of undoped GaN by a careful preparation which does not involve any magnetic impurities. We have also studied the magnetic properties of CdS, which is an important semiconductor exhibiting interesting nonlinear optical and luminescence properties.<sup>25</sup> Indeed, our results show that these nanoparticles are ferromagnetic at room temperature even without the substitution of magnetic elements. Similar to oxides, the origin of ferromagnetism has been suggested to be due to defects at the surface of the nanoparticles. In fact, electronic structural calculations have predicted that Ga vacancies in undoped GaN gives a ferromagnetic ground state.<sup>27</sup>

GaN nanoparticles were synthesized from metal trichloride-urea complex as reported earlier.<sup>28</sup> Gallium trichloride and urea form an isostructural complex with the *P-3c1* space group in which the metal is coordinated by six urea molecules. This complex on thermal decomposition above 800 °C in N<sub>2</sub> or NH<sub>3</sub> atmosphere yields GaN. One gram of Ga<sub>2</sub>O<sub>3</sub> (99.99%) was dissolved in concentrated HCl. Once a clear solution of GaCl<sub>3</sub> was formed, isopropyl alcohol (10 ml) was added. The desired amount of urea (99.5%) was added to the above solution and was continuously sonicated to obtain a white slurry and/or gel. The gel thus obtained was dried and decomposed at 850 °C and 950 °C in N<sub>2</sub> atmosphere. In order to obtain bulk GaN, the powder heated at 850 °C was pressed into a rectangular bar and sintered at 950 °C in NH<sub>3</sub> atmosphere for 12–16 hours.

CdS nanoparticles were synthesized by a simple sol-gel method.<sup>29</sup> About 30 mM mercaptoethanol was added to 50 ml of 30 mM CdCl<sub>2</sub> (95%) and stirred for 15 minutes. To this solution, 50 ml of 30 mM Na<sub>2</sub>S solution was added dropwise and the solution was stirred for 1 hour. The resulting solution was centrifuged to obtain the particles. To eliminate mercaptoethanol these particles were further washed three times with deionized water and finally with ethanol. The precipitate obtained after final centrifuge was dried overnight at room temperature, then annealed at 150 °C in N<sub>2</sub> atmosphere for 3 hours. To vary the particle size, the concentration of mercaptoethanol was varied (30 mM, 15 mM,

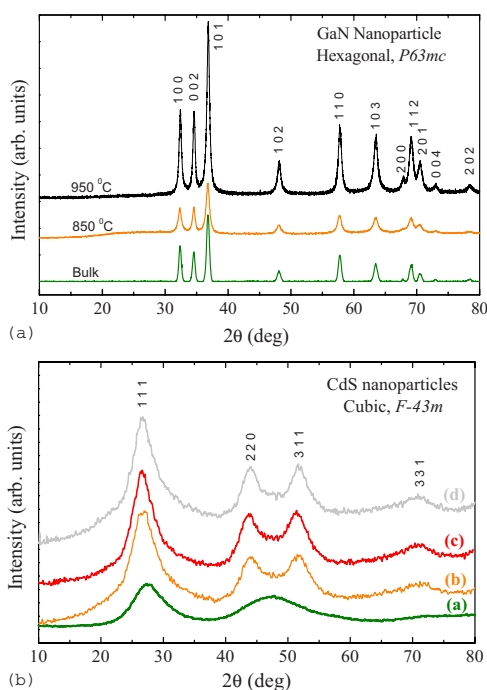


FIG. 1. (Color online) (a) XRD pattern of GaN nanoparticles annealed at different temperatures, 850 °C, 950 °C, and the bulk indicates the agglomerated particles (for details see text). (b) XRD pattern of CdS nanoparticles synthesized with different mercaptoethanol concentrations: (a) 30 mM as prepared, (b) 30 mM, (c) 15 mM, (d) without mercaptoethanol. The samples (b), (c), and (d) were annealed at 150 °C in  $N_2$  atmosphere.

3.75 mM, and without mercaptoethanol), while concentration of  $CdCl_2$  and  $Na_2S$  were kept constant.

The x-ray diffraction (XRD) pattern of GaN and CdS particles were recorded with a Rigaku-99 diffractometer using  $Cu K\alpha$  radiation ( $\lambda=1.5406 \text{ \AA}$ ). UV spectra were recorded on Perkin Elmer's Lambda900 spectrometer. To examine the morphology of particles, a field emission scanning electron microscopy (FESEM) (NOVA NANO600-FEI, The Netherlands) and transmission electron microscopy (TEM) (JEOL, JEM-3010 electron microscope) working at accelerating voltage of 300 kV were used. Electron paramagnetic resonance (EPR) spectra were recorded using a Bruker EMX X-band continuous wave (CW) EPR spectrometer. Magnetization measurements were performed using a vibrating sample magnetometer (VSM) option in the Physical Properties Measuring System (PPMS, Quantum Design, USA).

XRD patterns of GaN and CdS are shown in Figs. 1(a) and 1(b), respectively. The XRD pattern of GaN confirms the hexagonal structure (space group  $P63mc$ ) with the lattice parameters,  $a=3.19 \text{ \AA}$  and  $c=5.189 \text{ \AA}$ . It should be noted that no gallium oxide impurity was found. The XRD pattern of CdS nanoparticles is consistent with the cubic structure with the lattice parameter  $a=5.811 \text{ \AA}$  (space group  $F-43M$ ). In both cases, the broad diffraction peaks indicate smaller particle size.

Figures 2(a) and 2(c) display FESEM images of GaN particles heated at 850 °C, 950 °C, and bar annealed at 950 °C (bulk). The sample heated at 850 °C shows distribution of particles in the range 15–20 nm. The 950 °C heated sample

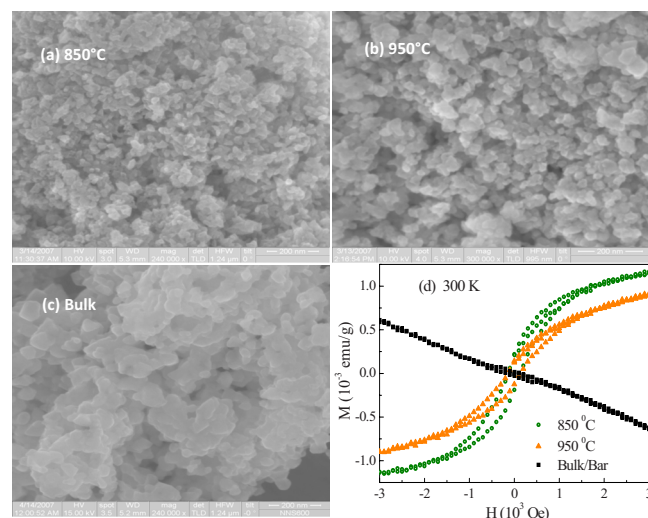


FIG. 2. (Color online) (a) and (b) are the FESEM image of GaN nanoparticles annealed at 850 °C and 950 °C, respectively. (c) FESEM image of the compressed particles (bar) annealed at 950 °C. (d) Room-temperature magnetization versus field curves for the three samples. The nanoparticles show ferromagnetism (magnetization corrected for the core diamagnetism), while the bulk exhibits diamagnetism.

has particles with slightly larger diameter (25–30 nm). This is in close agreement with the values obtained from the analysis of the x-ray diffraction profile using the Scherrer formula. The bulk GaN prepared by sintering the bar made from the 850 °C sample has agglomerated particles (the size of these agglomerates range from 150–350 nm) instead of micron size particles as it is difficult to sinter nitrides. Magnetization versus applied field  $M(H)$  data of these GaN particles recorded at room temperature are shown in Fig. 2(d). It can be seen that both 850 °C and 950 °C particles show ferromagnetic hysteresis, whereas the bulk or the agglomerated particles show diamagnetic behavior. It should be noted that the ferromagnetic hysteresis could be seen even at 390 K, indicating that the Curie temperature is quite high. With an increase of annealing temperature or the particle size the magnetic moment decreases. This behavior of magnetization with varying particle size is similar to that observed in nonmagnetic oxide nanoparticles.<sup>22</sup> This suggests that the ferromagnetism in GaN is essentially confined to the surface of the nanoparticles due to possible defects such as Ga or N vacancies. The magnetization saturates at around 3000 Oe, and at high fields the diamagnetic contribution from the core of the particles dominates and therefore the magnetization decreases with further increase of field. In order to show the surface magnetization, the diamagnetic contribution from the core of the nanoparticles is subtracted out and the resultant  $M(H)$  data are shown in Fig. 2(d). The saturation moment of 850 °C particles is  $\sim 1.2 \times 10^{-3} \text{ emu/g}$  and the coercivity is around 200 Oe. Both Ga and N vacancies are suggested to be present in the as-grown GaN depending on the growth conditions.<sup>30</sup> Calculations of the energies of formation of Ga and N vacancies in bulk GaN have been reported in the literature.<sup>17</sup> Although the formation of nitrogen vacancy has lower energy, electronic structure calculations have shown

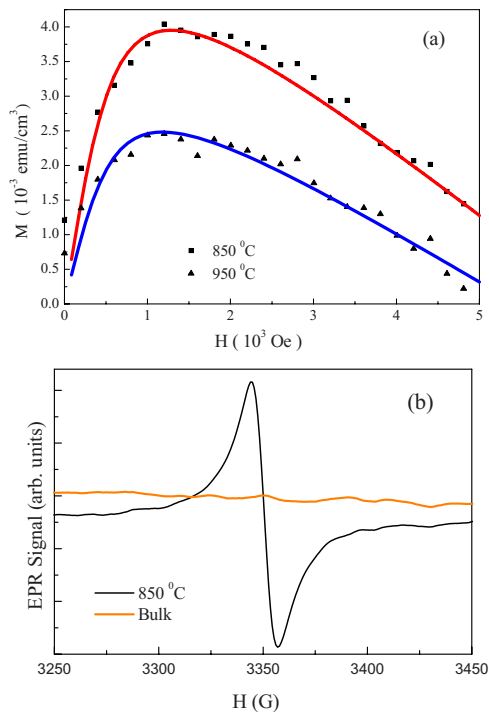


FIG. 3. (Color online) (a) Langevin fit to the magnetization data for GaN particles annealed at 850 °C and 950 °C. The lines are fit to the data. (b) EPR spectrum measured at 300 K for GaN particles annealed at 850 °C and bulk sample. The 850 °C annealed sample shows EPR signal with  $g=2.0047$ , while no signal is observed for bulk sample.

that this type of vacancy causes a paramagnetic state. On the other hand, Ga vacancies introduce magnetic moments which lie on the neighboring N atoms that are spin polarized due to Hund's rule.<sup>26,27</sup> This type of magnetism due to defects in bulk GaN has not been observed because of the large formation energy of defects in bulk GaN. However, the defect formation energy at the surface may be significantly different from that in the bulk due to the size effect which involves structural as well as electronic effects. Thus, the defect formation energies at the surface are lower, resulting in high concentration of defects which gives rise to percolative ferromagnetism at the surface of the nanoparticles of GaN. As the size of the particles increases, the defect concentration decreases and thus the magnetism vanishes.

We have analyzed the  $M(H)$  data using the well-known Langevin function which includes diamagnetic contribution to account for the core diamagnetic susceptibility. The fitted data using the relation  $M(H)=M_S L(x)+\chi_D H$ , where  $M_S$  is the saturation magnetization,  $L(x)=\coth(x)-1/x$  is the Langevin function,  $x=\mu_p H/kT$ ,  $\mu_p$  is the average moment per particle,  $k$  is the Boltzmann constant, and  $\chi_D$  is the diamagnetic susceptibility, is shown in Fig. 3(a). A good fit to the observed data confirms the existence of ferromagnetic correlations. The average moment per particle obtained from the fit for the 850 °C samples is  $18 \times 10^3 \mu_B$ , which is comparable to that observed for Sn nanoparticles.<sup>31</sup> Assuming that each defect contributes around  $2 \mu_B$ , we have estimated the number of defects to be around  $2 \times 10^{17} \text{ cm}^{-3}$ , which is very close to that reported for the electron irradiated GaN bulk.<sup>32</sup>

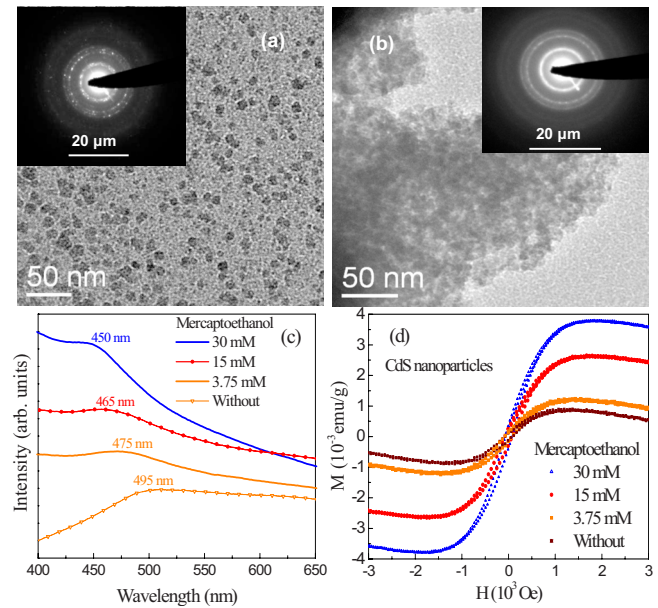


FIG. 4. (Color online) (a) TEM image of CdS nanoparticles of 15 mM mercaptoethanol capped, inset is the electron diffraction (ED) pattern of single particle and (b) TEM image of particles prepared without capping, showing agglomeration of particles. (c) UV absorption spectrum for CdS nanoparticles, the shift in the peak position is in agreement with particle size variation. (d) Room-temperature magnetization data for the various nanoparticles showing the highest saturation moment of  $4 \times 10^{-3} \text{ emu/g}$  for the 30 mM sample.

Results of EPR measurements at room temperature for the 850 °C annealed GaN sample and bulk GaN sample are shown in Fig. 3(b). It can be seen that the 850 °C heated particles show EPR signal whereas the bulk sample has no signal. The  $g$  value for the 850 °C annealed sample was calculated using the relation  $h\nu=g\mu_B H_0$ , where  $h$  is Planck's constant,  $\mu_B$  is Bohr magneton,  $H_0$  is the resonance field or central field of the signal from the sample, and  $\nu$  is the resonant frequency (9.4 GHz). The value of  $g$  is  $2.004 \pm 0.0005$ . EPR studies have been reported in the literature on GaN thin films and in a few cases on single crystals. For Mg-doped ( $p$ -type conductive) GaN the  $g$  value of  $g_{\parallel}=2.097 \pm 0.0015$  and  $g_{\perp}=1.994 \pm 0.004$  are assigned to Mg acceptors; for undoped GaN ( $n$ -type) crystals  $g_{\parallel}=1.9514 \pm 0.0005$  and  $g_{\perp}=1.9486 \pm 0.0005$  are ascribed to the shallow donor of GaN.<sup>33</sup> In the case of thermal annealed GaN crystals prepared by AMMONO method, the observed  $g=2.0026 \pm 0.0005$  was assigned to be due to deep acceptors.

As mentioned before, CdS nanoparticles were prepared using  $\text{CdCl}_2$  and  $\text{Na}_2\text{S}$  and mercaptoethanol as the stabilizer. To eliminate excess water, as-prepared CdS nanoparticles were heated at 150 °C. To obtain the decomposition details we performed thermogravimetric analysis and differential-thermal-conductivity analysis (TGA-DTA) of as-prepared CdS particles in  $\text{N}_2$  atmosphere. TGA-DTA measurements showed that water eliminates at around 100 °C and the nanoparticles partially oxidize in the temperature range 500–700 °C and form a mixed phase of CdO and CdS, as confirmed by x-ray diffraction.

TEM images of CdS nanoparticles are shown in Figs. 4(a) and 4(b), Fig. 4(a) displays the TEM image of nanoparticles prepared by using 15 mM mercaptoethanol, the particle size range is from 15–20 nm. The inset in Fig. 4(a) displays the electron diffraction pattern of a single particle which reveals the polycrystalline nature of the particles. The particle size of sample obtained from 0.03M mercaptoethanol varied from 10–12 nm. TEM image of CdS nanoparticles prepared without stabilizer is shown in Fig. 4(b), where the particles are agglomerated. One can observe that the particle size increases by decreasing mercaptoethanol concentration, and when no capping agent is used the particles are bigger (>25 nm) and also they agglomerate. We also noted that the color of the samples varied from yellow (30 mM), orange (15 mM), to light brown (without stabilizer) confirming the size variation. Further, UV absorption spectra [Fig. 4(c)] show that there is a redshift of absorption peak with increasing particle size.

Figure 4(d) displays the results of magnetic measurements

on CdS nanoparticles at room temperature. While all the samples show ferromagnetic behavior with coercive field in the range 100–150 Oe, the smaller particles show the largest magnetization ( $\sim 4 \times 10^{-3}$  emu/g) and with increasing particle size, the magnetization decreases. Though the saturation magnetic moment observed in both GaN and CdS is small, it is comparable to that in the case of nonmagnetic oxides.<sup>22</sup>

We have demonstrated that undoped GaN and CdS nanoparticles show room-temperature ferromagnetism, exhibiting an increase in saturation magnetic moment with the decrease in particle size. Agglomerated bigger particles show diamagnetism or a weak ferromagnetism. The origin of ferromagnetism has been discussed in terms of defects at the surface of the nanoparticles. This observation is of much relevance to the field of dilute magnetic semiconductors.

The authors thank Usha Tumkurkar for the TEM, N. R. Selvi for the FESEM images, and S. V. Bhat for EPR measurements.

\*sundaresan@jncasr.ac.in

†cnrrao@jncasr.ac.in

- <sup>1</sup>T. Dietl, H. Ohono, F. Matsukar, J. Cibert, and D. Ferrand, *Science* **287**, 1019 (2000).
- <sup>2</sup>Q. Wang, Q. Sun, and P. Jena, *Phys. Rev. Lett.* **95**, 167202 (2005).
- <sup>3</sup>G. T. Thaler, M. E. Overberg, B. Gila, R. Frazier, C. R. Abernathy, S. J. Pearton, J. S. Lee, S. Y. Lee, Y. D. Park, Z. G. Khim, J. Kim, and F. Ren, *Appl. Phys. Lett.* **80**, 3964 (2002).
- <sup>4</sup>K. Sardar, A. R. Raju, B. Bansal, V. Venkataraman, and C. N. R. Rao, *Solid State Commun.* **125**, 55 (2003).
- <sup>5</sup>Han-Kyu Seong, Jae-Young Kim, Ju-Jin Kim, Seung-Cheol Lee, So-Ra Kim, Ungkil Kim, Tae-Eon Park, and Heon-Jin Choi, *Nano Lett.* **7**, 3366 (2007).
- <sup>6</sup>C. Xu, J. Chun, K. Rho, D. E. Kima, B. J. Kim, S. Yoon, S.-E. Han, and J.-J. Kim, *J. Appl. Phys.* **99**, 064312 (2006).
- <sup>7</sup>K. Ando, *Appl. Phys. Lett.* **82**, 100 (2003).
- <sup>8</sup>P. P. Chen, H. Makino, J. J. Kim, and T. Yao, *J. Cryst. Growth* **251**, 331 (2003).
- <sup>9</sup>M. Zajac, R. Doradzinski, J. Gosk, J. Szczytko, M. Lefeld-Sosnowska, M. Kaminska, A. Twardowski, M. Palczewska, E. Grzanka, and W. Gebicki, *Appl. Phys. Lett.* **78**, 1276 (2001).
- <sup>10</sup>Alberta Bonanni, Michal Kiecana, Clemens Simbrunner, Tian Li, Maciej Sawicki, Matthias Wegscheider, Martin Quast, Hanka Przybylińska, Aandrea Navarro-Quezada, Rafal Jakiela, Agnieszka Wolos, Wolfgang Jantsch, and Tomasz Dietl, *Phys. Rev. B* **75**, 125210 (2007).
- <sup>11</sup>M. Zajac, J. Gosk, E. Grzanka, M. Kaminska, A. Twardowski, B. Strojek, T. Szyszko, and S. Podsiadlo, *J. Appl. Phys.* **93**, 4715 (2003).
- <sup>12</sup>S. Sonoda, I. Tanaka, H. Ikeno, T. Yamamoto, F. Oba, T. Araki, Y. Yamamoto, K. Suga, Y. Nanishi, Y. Akasaka, K. Kindo, and H. Hori, *J. Phys.: Condens. Matter* **18**, 4615 (2006).
- <sup>13</sup>G. P. Das, B. K. Rao, and P. Jena, *Phys. Rev. B* **68**, 035207 (2003).
- <sup>14</sup>K. Biswas, K. Sardar, and C. N. R. Rao, *Appl. Phys. Lett.* **89**, 132503 (2006).
- <sup>15</sup>M. Venkatesan, C. B. Fitzgerald, and J. M. D. Coey, *Nature* (London) **430**, 630 (2004).
- <sup>16</sup>N. H. Hong, J. Sakai, N. Poirrot, and V. Brizé, *Phys. Rev. B* **73**, 132404 (2006).
- <sup>17</sup>S. Limpijumngong and C. G. Van de Walle, *Phys. Rev. B* **69**, 035207 (2004).
- <sup>18</sup>S. D. Yoon, Y. Chen, A. Yang, T. L. Goodrich, X. Zuo, D. A. Arena, K. Ziemer, C. Vittoria, and Vincent G. Harris, *J. Phys.: Condens. Matter* **18**, L355 (2006).
- <sup>19</sup>N. H. Hong, J. Sakai, and V. Brizé, *J. Phys.: Condens. Matter* **19**, 036219 (2007).
- <sup>20</sup>N. H. Hong, N. Poirrot, and J. Sakai, *Phys. Rev. B* **77**, 033205 (2008).
- <sup>21</sup>J. Osorio-Guillén, S. Lany, S. V. Barabash, and A. Zunger, *Phys. Rev. B* **75**, 184421 (2007).
- <sup>22</sup>A. Sundaresan, R. Bhargavi, N. Rangarajan, U. Siddesh, and C. N. R. Rao, *Phys. Rev. B*, **74**, 161306(R) (2006).
- <sup>23</sup>Shipra, A. Gomathi, A. Sundaresan, and C. N. R. Rao, *Solid State Commun.* **142**, 685 (2007).
- <sup>24</sup>R. V. K. Mangalam, Nirat Ray, U. V. Waghmare, A. Sundaresan, and C. N. R. Rao (unpublished).
- <sup>25</sup>W. Wang, I. Germanenko, and S. El-Shall, *Chem. Mater.* **14**, 3028 (2002).
- <sup>26</sup>P. Larson and S. Satpathy, *Phys. Rev. B* **76**, 245205 (2007).
- <sup>27</sup>P. Mahadevan and S. Mahalakshmi, *Phys. Rev. B* **73**, 153201 (2006).
- <sup>28</sup>K. Sardar, M. Dan, B. Schwenzer, and C. N. R. Rao, *J. Mater. Chem.* **15**, 2175 (2005).
- <sup>29</sup>W. Vogel, P. H. Borse, N. Deshmukh, and S. K. Kulkarni, *Langmuir* **16**, 2032 (1999).
- <sup>30</sup>Chris G. Van de Walle and J. Neugebauer, *J. Appl. Phys.* **95**, 3851 (2004).
- <sup>31</sup>W.-H. Li, C.-W. Wang, C.-Y. Li, C. K. Hsu, C. C. Yang, and C.-M. Wu, *Phys. Rev. B* **77**, 094508 (2008).
- <sup>32</sup>K. Saarinen, T. Suski, I. Grzegory, and D. C. Look, *Phys. Rev. B* **64**, 233201 (2001).
- <sup>33</sup>M. Palczewska, B. Suchanek, R. Dwilinski, K. Paku, A. Wagner, and M. Kaminska, *MRS Internet J. Nitride Semicond. Res.* **3**, 45 (1998).